

# Spatiotemporal Self-Organization upon Two-Wave Mixing in a Photorefractive Medium

P. A. Prudkovskii

Faculty of Physics, Moscow State University, Vorob'evy gory, Moscow, 119992 Russia

e-mail: pasha@qopt.phys.msu.su

Received 2003

Nonlinear dynamics of recording volume holographic gratings upon two-wave mixing in an inertial photorefractive media were studied. It is found that the space–time dependence of the grating diffraction efficiency can be quasi-regular, allowing the understanding of the experimentally observed irregular behavior of the diffracted light intensity. © 2003 MAIK “Nauka/Interperiodica”.

PACS numbers: 42.40.Pa; 42.40.Lx; 42.70.Nq; 42.65.Hw

Investigations into photorefraction, i.e., into the processes of light-induced change in the refractive index of a medium, have allowed one to discover many new photorefractive materials in the last several decades and find numerous applications for them [1, 2]. However, with the development of the hologram record technique and information storage in such media, it has become clear that wave-mixing processes may be much more complicated than was assumed previously [3].

In this work, we discuss certain features of wave mixing in a photorefractive medium in the course of recording volume holographic grating by two crossing light beams. The time dependence of the diffraction efficiency of the recorded grating, as a rule, is smooth and practically monotonic at low light intensities or in media with weak photorefractive nonlinearity [4, 5]. However, an increase in the light intensity or the use of stronger nonlinearities may be accompanied by sharp differentials in the diffraction efficiency and their sensitivity to the experimental conditions. In this work, it is shown that such a jumpwise behavior of diffraction efficiency of a volume holographic grating is a consequence of the formation of a regular spatiotemporal structure in the course of recording grating in an inertial photorefractive medium.

**Description of the model.** We consider the standard model of recording holographic grating in a medium with photorefractive response. Two coherent light beams intersect in a medium to form an interference pattern. Due to the diffusion or photovoltaic effect, the electric-charge carriers are rearranged in the medium to produce an electrostatic field which modulates the refractive index through the electrooptical effect. Therefore, the state of light and medium is specified by three complex field variables: slowly varying field amplitudes of two beams  $E_{1,2}(x, t)$  and spatially oscillating amplitude of electrostatic field  $\mathcal{E}(x, t)$ . In the approximation of a perfectly transparent medium, their

spatiotemporal evolution is described by a set of partial differential equations, which can be written in the form [6–8]

$$\begin{aligned} \frac{\tau_m \partial \mathcal{E}}{\partial t} + \mathcal{E} &= \gamma E_1, E_2^*, \\ \frac{\partial E_2}{\partial x} &= i\mathcal{E}^* E_1, \quad \frac{\partial E_1}{\partial x} = i\mathcal{E} E_2, \end{aligned} \quad (1)$$

where  $\tau_m = \varepsilon/4\pi\sigma$  is the characteristic Maxwellian response time of the medium,  $\varepsilon$  is its dielectric constant,  $\sigma$  is conductivity, and  $\gamma = Ge^{i\varphi}$  is the effective photorefractive coefficient, which includes a combination of the photovoltaic and electrostatic tensor components and the diffusion coefficient.

From the second and third equations, it follows that the total light intensity in the system is constant:  $|E_1|^2 + |E_2|^2 = \text{const} = I_0$ . Taking into account this conservation law, it is convenient to make the change of variables  $E_1 = \sqrt{I_0} e^{i\psi_1} \cos(\beta/2)$  and  $E_2 = \sqrt{I_0} e^{i\psi_2} \sin(\beta/2)$ . In the new variables, system (1) takes the form

$$\begin{aligned} \frac{\partial \mathcal{L}}{\partial \tau} + \mathcal{L} &= \sin \beta e^{-i\psi}, \\ \frac{\partial \beta}{\partial y} - i \tan \beta \frac{\partial \psi}{\partial y} &= -i\mathcal{L} e^{i(\psi + \varphi)}, \end{aligned} \quad (2)$$

where the variables  $\mathcal{L} = 2\mathcal{E}/\gamma I_0$ ,  $\psi = \psi_2 - \psi_1$ , and new time and length scales

$$\tau = t/\tau_m, \quad y = GI_0 x \quad (3)$$

are introduced. Therefore, the behavior of the system depends qualitatively on a single parameter  $\varphi$ , which determines the ratio between the real and imaginary components of the photorefractive coefficient  $\gamma$ . The behavior of all remaining parameters can be taken into

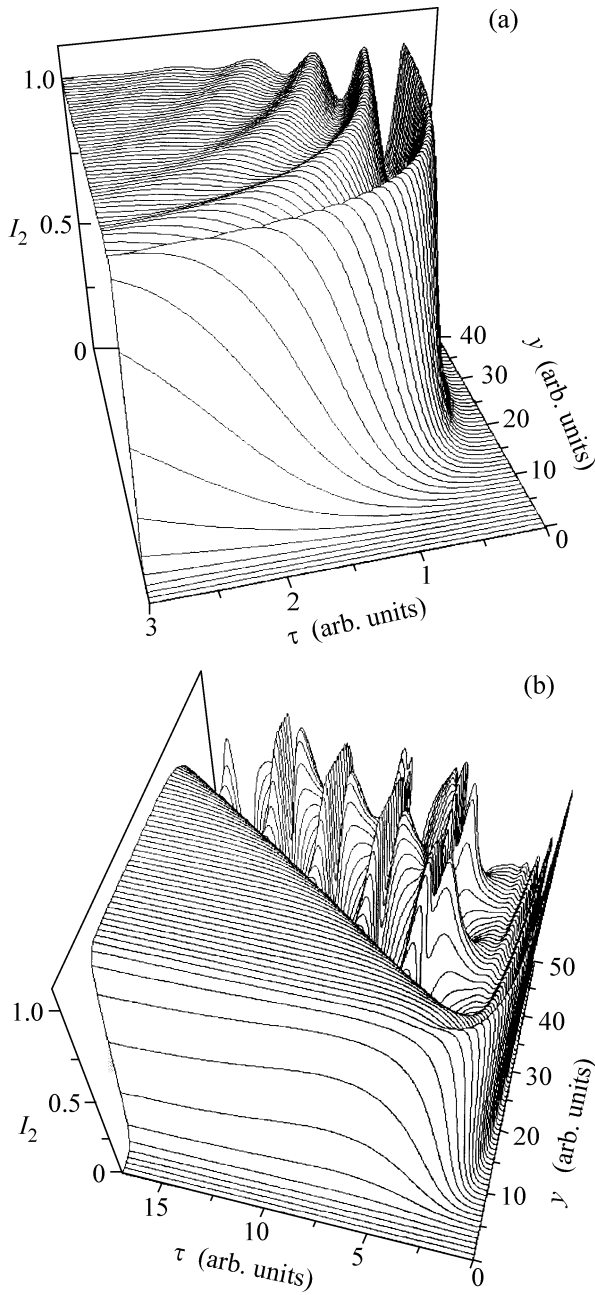


**Fig. 1.** Three-dimensional intensity profile for the secondary light beam  $I_2$  as a function of time  $\tau$  and thickness  $y$  of the photorefractive medium for (a) purely imaginary coefficient  $\gamma$  of photorefractive nonlinearity ( $\varphi = \pi/2$ ) and (b) equal real and imaginary parts of this coefficient ( $\varphi = \pi/4$ ).

account by changing the space and time scales. In particular, the variation of light intensity  $I_0$  is equivalent to changing the thickness of photorefractive medium.

It is known [9, 10] that the recorded holographic grating for real  $\gamma$  is not shifted relative to the interference pattern. In this case, stationary energy exchange is impossible; after the termination of recording grating,

the beam intensities in the photorefractive medium are not rearranged. In all other cases, the intensity of one beam will transfer to another (in our notation, energy transfer occurs from the first to the second beam if  $0 < \varphi < \pi$ ).

In the case of imaginary photorefractive nonlinearity  $\varphi = \pi/2$  (which corresponds, in particular, to the diffusional photorefraction mechanism), the system can be simplified, because there is a stable solution of the form  $\arg \mathcal{E} = \pi n - \psi = \text{const}$ . The rest of the set of Eqs. (2) amounts to the equation

$$\frac{\partial^2 \beta}{\partial y \partial \tau} + \frac{\partial \beta}{\partial \tau} = \sin \beta, \quad (4)$$

which has the form of a modified sine-Gordon equation with the additional first derivative. The analytic solution to this equation and to the complete set of Eqs. (2) cannot be found. For this reason, we present here only numerical solutions.

**Results of numerical integration.** The set of Eqs. (2) consists of four real equations, two of which contain only time derivatives and the other two contain only spatial derivatives. Due to this, one can easily develop a computational algorithm based on the numerical integration of the two parts of system (2), similar to the usual differential equations, to obtain the solution by specifying the intensity ratio  $I_2/I_1|_{y=0} \equiv I_{02}/I_{01} = \tan(\beta_0/2)$  and phase difference  $\psi|_{y=0} \equiv \psi_0$  for two light beams at the medium input as boundary conditions and the absence of electrostatic field  $\mathcal{E}$  at  $\tau = 0$  as the initial condition. The numerical integration gave the spatiotemporal dependences for the second-beam intensity normalized to the total intensity  $I_0$ , with the boundary conditions  $\psi_0 = 0$ ,  $I_{02}/I_0 = 10^{-4}$  and various phases of the photorefractive nonlinearity coefficient  $\varphi$ . For such a low initial input intensity of the second beam, its output intensity is a measure of the diffraction efficiency of the recorded grating.

Figure 1a shows the three-dimensional intensity profile of the second beam for the imaginary coefficient  $\gamma$  ( $\varphi = \pi/2$ ). It demonstrates the dependence of intensity on both time and length. One can see that the obtained solution describes a smooth increase in the intensity of the second beam at the output of photorefractive medium with small damping oscillations near the maximum. This is precisely the behavior that was considered classical for the processes of recording holograms and photoinduced light scattering at the dawn of photorefractive [5].

However, in the general case, the behavior of light intensity at the output of the photorefractive medium may be much more complicated. Figure 1b shows the three-dimensional intensity map for the second beam in the case of  $\gamma$  with equal real and imaginary parts ( $\varphi = \pi/4$ ). One can see that the evolution of beam intensity at short lengths is almost the same as in the case of imaginary  $\gamma$ . Recall that, on the scale adopted, the effective

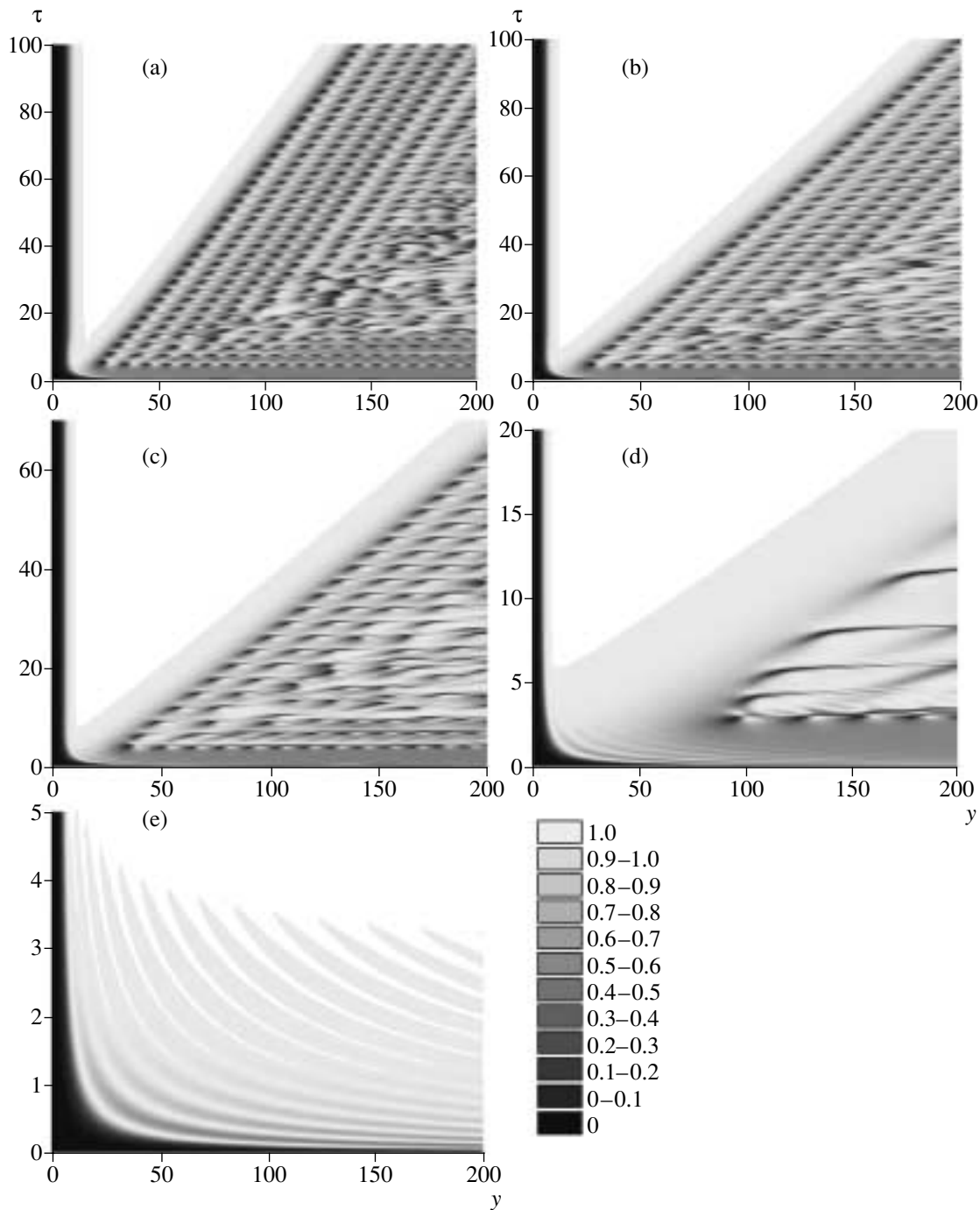


**Fig. 2.** Two-dimensional intensity distribution for the second beam  $I_2$  as a function of time  $\tau$  and thickness  $y$  of the photorefractive medium for different phases  $\varphi$  of the photorefractive nonlinearity coefficient  $\gamma$ :  $\varphi =$  (a)  $\pi/5$ , (b)  $\pi/4$ , (c)  $3\pi/10$ , (d)  $2\pi/5$ , and (e)  $\pi/2$ .

length unit depends both on the total light intensity and on the magnitude of photorefractive nonlinearity (3). Since the laser intensity in the early studies of photorefraction was too low to produce a strong light field, the effective thicknesses of photorefractive media were rather small, so that almost all observed dependences were smooth and monotonic. However, for the larger interaction lengths (or beam intensities), the time

dependences contain a strongly fluctuating region, whose length increases approximately proportional to the interaction length.

Let us consider a set of spatiotemporal dependences for the intensity of second beam and various values of phase  $\varphi$ . The corresponding dependences are shown in Fig. 2 in the form of two-dimensional brightness distributions (Fig. 2a corresponds to Fig. 1a, and Fig. 2d cor-

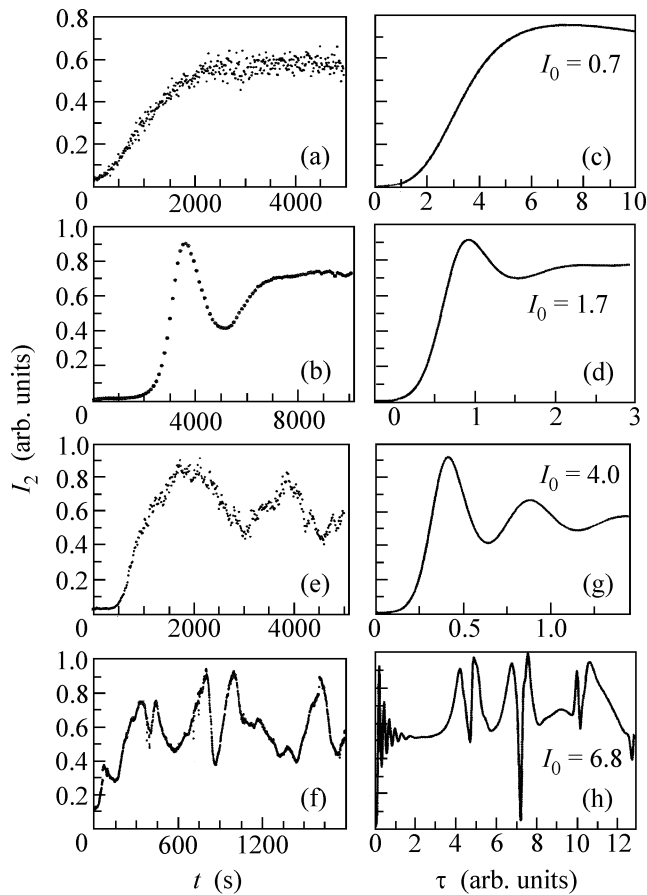


**Fig. 3.** Comparison of the experimental time dependences of the intensity  $I_2$  of the second beam (a, b, e, f) with the analogous theoretical dependences for different total light intensities  $I_0$  (c, d, g, h).

responds to Fig. 1b). One can see that, if the photorefractive coefficient has a nonzero real part, the whole  $\tau$ - $y$  plane can be separated into two regions divided by a near-straight line emerging from the origin of coordinates. In the upper part adjacent to the time axis, the intensity  $I_2$  rapidly and more or less monotonically increases and becomes saturated at  $I_2 = I_0$ . At the same time, the two-dimensional structure formed in the region adjacent to the spatial axis is rather complicated and has a regular quasiperiodic character. It should be noted that the slope of the line separating the regions increases with decreasing phase  $\varphi$ .

Let us now compare these results with the experimental data.

**Comparison with experiment.** The experimental curves presented below were obtained while studying two-wave mixing, photoinduced light scattering, and parametric scattering of holographic type in photorefractive copper-doped lithium niobate crystals [11, 12]. Two light beams were brought together in a photorefractive crystal, with the intensity of one of them being approximately four orders of magnitude higher than for

the other. The Maxwellian time in such crystals equals several tens of minutes and decreases with increasing light intensity because of an increase in the photoelectron conductivity. As the process of holographic grating evolves, the intensity of the first beam is partly transferred to the second beam.

To compare with the experimental data, the  $I_2(\tau)$  dependences were extracted from the complete solution to Eqs. (2) with various effective thicknesses of the photorefractive medium.

The experimental curves for the intensity  $I_2$  of the second beam at the output of a photorefractive crystal are shown in Figs. 3a and 3b for relatively low intensities of the first beam, and the appropriate theoretical curves obtained for various effective thicknesses are shown in Figs. 3c and 3d. As was pointed out above, the length scale depends on the total light intensity; because of this, the increase in the effective thickness corresponds to the increase in the intensity of the first beam for a fixed crystal thickness. Figures 3e and 3f and Figs. 3g and 3h show, respectively, the corresponding theoretical curves for higher intensities of the first beam;  $I_1$  in Fig. 3e is higher than the intensity of the first beam in Fig. 3a by almost an order of magnitude, and  $I_1$  in Fig. 3e is one order of magnitude higher than the analogous intensity in Fig. 3b. It is seen from these graphs that the theoretical curves obtained by the numerical integration of Eqs. (2) describe not only the smooth evolution of the energy-exchange process at low intensities but also the sharp changes in the diffraction efficiency of holographic grating at high light intensities or large thicknesses of the photorefractive medium (Fig. 3e).

Thus, it is shown in this work that the spatiotemporal dependence of the diffraction efficiency of a holographic grating may have a complex quasi-regular structure if the coefficient of photorefractive nonlinearity is complex and the pumping is strong enough (Fig. 2). This is manifested experimentally in the form of sharp intensity differences in the intensity of diffracted light (Fig. 3e). The boundary of this structure in the  $\tau$ - $y$  plane is a straight line emerging from the origin of coordinates. Its slope depends on the phase of the coefficient of photorefractive nonlinearity. This, in principle, provides an original method of measuring the ratio between the real and complex parts of the photovoltaic tensor components.

This work was supported by the Russian Foundation for Basic Research (project no. 02-02-16843) within the framework of the program "Fundamental Optics and Spectroscopy."

## REFERENCES

1. T. R. Volk, N. V. Razumovski, A. V. Mamaev, and N. M. Rubinina, *J. Opt. Soc. Am. B* **13**, 1457 (1996).

2. V. A. Vysloukh, V. Kutuzov, and V. V. Shuvalov, *Kvantovaya Élektron. (Moscow)* **23**, 157 (1996).
3. V. A. Vysloukh, V. Kutuzov, V. M. Petnikova, and V. V. Shuvalov, *Zh. Éksp. Teor. Fiz.* **111**, 705 (1997) [JETP **84**, 388 (1997)].
4. F. S. Chen, J. T. La Macchia, and D. V. Fraser, *Appl. Phys. Lett.* **13**, 223 (1968).
5. K. N. Zabrodin and A. N. Penin, *Kvantovaya Élektron. (Moscow)* **18**, 622 (1991).
6. M. Cronin-Golomb, J. O. White, B. Fisher, and A. Yariv, *Opt. Lett.* **7**, 313 (1982).
7. A. Novicov, S. Odoulov, O. Oleinik, and B. Sturman, *Ferroelectrics* **66**, 1 (1986).
8. P. A. Prudkovskii, O. V. Skugarevskii, and A. N. Penin, *Vestn. Mosk. Univ., Ser. 3: Fiz., Astron.* **5**, 38 (1998).
9. B. Ya. Zel'dovich, *Kratk. Soobshch. Fiz.* **5**, 20 (1970).
10. V. L. Vinetskiĭ, N. V. Kukhtarev, S. G. Odulov, and M. S. Soskin, *Usp. Fiz. Nauk* **129**, 113 (1979) [*Sov. Phys. Usp.* **22**, 742 (1979)].
11. P. A. Prudkovskii, O. V. Skugarevskii, and A. N. Penin, *Zh. Éksp. Teor. Fiz.* **112**, 1490 (1997) [JETP **85**, 812 (1997)].
12. P. A. Prudkovskii and A. N. Penin, *Pis'ma Zh. Éksp. Teor. Fiz.* **70**, 660 (1999) [JETP Lett. **70**, 673 (1999)].

*Translated by V. Sakun*